

# Complexity and synchronization in stochastic chaotic systems

Thai Son Dang<sup>1</sup>, Sanjay Kumar Palit<sup>2</sup>, Sayan Mukherjee<sup>3</sup>, Thang Manh Hoang<sup>1</sup>,  
and Santo Banerjee<sup>4,a</sup>

<sup>1</sup> School of Electronics and Telecommunications, Hanoi University of Science and  
Technology, 01 Dai Co Viet, Hanoi, Vietnam

<sup>2</sup> Basic Sciences and Humanities Department, Calcutta Institute of Engineering and  
Management, Kolkata, India

<sup>3</sup> Department of Mathematics, Sivanath Sastri College, Kolkata, India

<sup>4</sup> Institute for Mathematical Research, Universiti Putra Malaysia, Selangor, Malaysia

Received 25 September 2015 / Received in final form 11 January 2016  
Published online 29 February 2016

**Abstract.** We investigate the complexity of a hyperchaotic dynamical system perturbed by noise and various nonlinear speech and music signals. The complexity is measured by the weighted recurrence entropy of the hyperchaotic and stochastic systems. The synchronization phenomenon between two stochastic systems with complex coupling is also investigated. These criteria are tested on chaotic and perturbed systems by mean conditional recurrence and normalized synchronization error. Numerical results including surface plots, normalized synchronization errors, complexity variations etc show the effectiveness of the proposed analysis.

## 1 Introduction

The complex real world phenomena can be classified into two categories – deterministic and stochastic. The deterministic phenomena often evolve in such a manner that in long term they becomes almost unpredictable. This type of behavior generally leads to chaos or hyperchaos. In fact, hyperchaos is more disordered than chaos. On the other hand, stochastic phenomena are non-deterministic due to the presence of randomness. Thus for all kinds of real world phenomena, some sort of uncertainty is always being there. Obviously, for a stochastic phenomenon it is more than a deterministic phenomenon. This actually means that as the system becomes more and more random, the amount of uncertainty gradually increases. This is measured by entropy, first introduced by C.E. Shannon [1]. More is the entropy value, more uncertainty is there in the corresponding phenomenon. The term complexity is used in this context. In general complexity is positively correlated with entropy. Since the inception of Shannon entropy, several entropy measures have been developed. Among those measures, Rennie's entropy [2] – a generalization of Shannon entropy, Kolmogorov-Sinai

<sup>a</sup> e-mail: santoban@gmail.com

entropy [3,4], approximate entropy (ApEn)[5], Sample entropy (SampEn)[6] have been used widely in diverse domains of research. After the introduction of the recurrence plots (RP) [12–15], few other measures of complexity [16] have been introduced. All of these measures were found to be more effective even than the Lyapunov exponent for the determination of the divergence behavior of dynamical systems [16–18]. Such entropy based quantifiers of RP's include normalized entropy of recurrence times [16] or the Shannon entropy of the distribution of length of diagonal line segments [16,17,19]. However, the major limitation of these RP based measures is that they all depend on the choice of the distance threshold for the construction of RP. This limitation is overcome in a recently introduced entropy measure based on weighted recurrence plot (WRP)[20]. In WRP, the choice of proper threshold is not required at all. So the entropy based on this WRP (WRPE) is expected to be more robust.

The calculation of all of the aforesaid entropy measures is generally done either from the phase space or from the reconstructed phase space [6] of the respective phenomenon. If the dynamical model exist then the entropy is computed directly from its phase space. However, as for most of the real world phenomena, proper dynamical model is not available, the entropy is calculated from its reconstructed phase space. Takens [7] proved that such reconstruction, if done with proper time-delay and suitable embedding dimension is equivalent to the original phase space. The embedding dimension is generally calculated by false nearest neighbor method. For determining the proper time-delay, various measures have been developed that includes auto-correlation, cross auto-correlation [8], new types of nonlinear auto-correlation of bivariate data [9], average mutual information (AMI) [10] and such others.

Synchronization on the other hand, is defined as a general process wherein two (or many) dynamical systems are coupled or forced (periodically or noisy), in order to realize a collective or synchronous behavior. Recently, investigation of synchronous phenomenon in coupled chaotic systems for the purposes of security is of interest of many researchers [22]. Among different kinds of synchronization in coupled complex systems, the mostly used types are Complete Synchronization (CS) [23–25], Generalized Synchronization (GS) [26,27] and Phase Synchronization (PS) [28,29]. CS is mainly studied only for the coupled identical systems, while for two non-identical systems, PS and GS are considered. Both of PS and GS can be described by the recurrences and joint recurrences between the trajectories of different systems. This is because if two systems are synchronized then obviously their recurrences are dependent to each other. The existence of the unidirectional coupling is measured by mean conditional recurrence (MCR) [30], which can also detect the driver and response systems in such coupling. MCR is basically the mean conditional probabilities of recurrence between the systems  $X$  and  $Y$ . It is computed from the recurrence plot (RP) and joint recurrence plot (JRP) [31].

In this article, our primary objective is to observe the behavior of a hyperchaotic system, when perturbed by some external sources like random noise, nonlinear and non-stationary music signals, speech signals or combination of both. In a more detail, we want to check whether or not the system shows a tendency for being stochastic with the increase of at least one of the system parameter responsible for the hyperchaos. The secondary objective is to check the synchronous behavior, if any, of the same hyperchaotic system when influenced by the aforesaid external sources and also to determine the nature of coupling.

## 2 Measure of complexity

Complexity is a term associated with a complex or complex adaptive system, which measures the amount of information related to the dynamics. Complex system is one,

which has many interacting components that make the whole unit highly nonlinear. It evolves over time with various interacting parameters; small changes in the parameters can make the system chaotic. For example, the dynamics of an organization is in general complex (not necessarily chaotic). The healthy human heart is complex, since it has many interacting subunits to keep the whole system (heart) active. A cardiac heart is less complex, since it fails to working properly with each interacting subunits [21].

Complexity of a system is generally understood by computing entropy of that system. Entropy actually measures the amount of uncertainty in a system. It increases when the system is more likely random and decreases, when it is less random. Thus, if the entropy is high for some system, the system is considered more complex, while for low entropy value, the system is less complex. Among different entropy measures, Shannon entropy, Kolmogorov-Sinai entropy have got tremendous response in the research communities. Since the inception of the recurrence plots (RP), few other measures of complexity have been introduced, which stand as more effective than the Lyapunov exponent in determining the divergence behavior of dynamical systems. Such entropy based quantifiers of RP's includes normalized entropy of recurrence times or the Shannon entropy of the distribution of length of diagonal line segments, which can detect points of bifurcation. However, these RP based entropy, sometimes fail to capture the complexity of the system properly because of the choice of improper distance threshold to obtain the binary recurrent matrix. Thus, an alternative notion of Weighted RP (WRP) was introduced. The Shannon entropy based on WRP is known as Entropy of the WRP (WRPE).

## 2.1 Entropy of the weighted recurrence plot

WRP, introduced by Deniz Eroglu et al. [20] is constructed just by considering the distances between the points in the phase space. The distance matrix  $W_{ij}$  is defined as  $W_{ij} = \|x_i - x_j\|, i, j = 1, 2, 3, \dots, N$ , where  $\|\cdot\|$  is the Euclidean norm of the reconstructed phase space. Unlike binary recurrent matrix  $R$ , which provides information on whether or not two points  $x_i$  and  $x_j$  are close in a  $n$ -dimensional phase space (say),  $\mathbf{W}$  only represents the distances between every pair of points of the time series. Thus in order to consider the proximity between points of the time series, the weighted matrix  $\tilde{W}$  is defined as

$$\tilde{W}_{ij} = e^{-\|x_i - x_j\|}. \quad (1)$$

In (1), the inverse of the exponential function has been considered because it scales the distances to the interval  $[0, 1]$ , where 0 and 1 respectively indicate the distant and close states. The advantage of this concept lies in the fact that without choosing a threshold the proximity of the phase space trajectory points can be described. To define the Shannon entropy based on this WRP, first the strength  $s_i$  of a point  $x_i$  in the phase space is calculated as

$$s_i = \sum_{j=1}^N \tilde{W}_{ij}. \quad (2)$$

$s_i$  basically quantifies the heterogeneity of the density of a given point in the phase space, which characterizes the amount of statistical disorder in the system through its distribution  $P(s)$ . This heterogeneity is calculated by the associated Shannon entropy of weighted matrix  $\tilde{W}$  given by

$$H = - \sum_{\{s\}} p(s) \ln(p(s)), \quad (3)$$

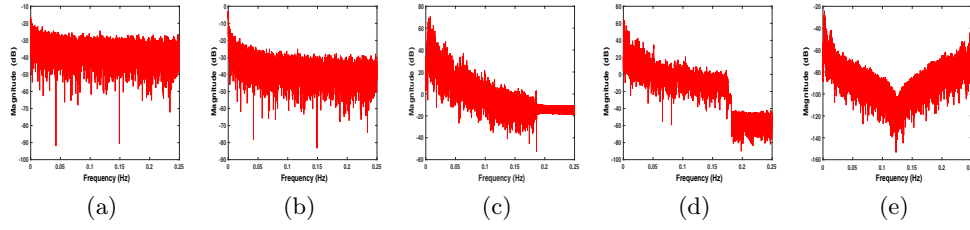


**Fig. 1.** The Power spectrum of the induced (a) power noise  $\frac{1}{f^{\beta_1}}, \beta_1 = 0.5$ , (b) power noise  $\frac{1}{f^{\beta_2}}, \beta_2 = 1$ , (c) music signal of traditional Vietnamese instrumental ( $m_1$ ), (d) music signal of raga Dagar ( $m_2$ ), and (e) speech signal ( $s_1$ ).

where  $p(s) = P(s)/S$  is the relative frequency distribution of the distance matrix strength and  $S = \sum_i^N s_i$  is the total number of strengths. This WRP based entropy ( $H$ ) has certain advantages over the entropy measures based on RP. First of all,  $H$  measures the complexity of scalar distributions (the strength  $s_i$ ) for each time point instead of measuring the complexity of distributions of the diagonals, which produces the border effect, results in deceptive entropy values. Secondly, as  $H$  considers all time points, the results are not biased by the number of diagonals and hence the time series length and the recurrence threshold are not crucial as in the case of entropy based on RP.  $H$  only depends on the estimation of  $p(s)$ , i.e., the chosen binning. Moreover,  $H$  is more correlated with the Lyapunov exponent than the RP based entropy. This is because, for periodic or stochastic dynamics, the strength  $s_i$  is found to be very similar for all time points, resulting in a confined distribution of  $p(s)$  and hence a very low entropy value, while for chaotic dynamics, the strength  $s_i$  varies strongly for different time points produces broad distribution of  $p(s)$  and a very high entropy value. In fact, these features are all successfully verified in [20] for the discrete logistic map, the continuous Rössler oscillator, and on experimental electrochemical data.

## 2.2 Computation of WRP entropy for the Lorenz-Stenflo and perturbed Lorenz-Stenflo systems

We now compute the WRP based entropy,  $H$  described above to find the changes in complexity of the four dimensional Lorenz-Stenflo (LS) system with respect to the system parameter  $r$ , when perturbed with two different noises or two different music signals or even with a combination of music and speech signals. The noises are basically power noise  $n_i = \frac{1}{f^{\beta_i}}, i = 1, 2$ ; with  $\beta_1 = 0.5, \beta_2 = 1$ . The music signal  $m_1$  is the recorded traditional Vietnamese instrumental, while the other music signal  $m_2$  is the recorded Indian classical music of raga Dagar. The speech signal,  $s_1$  is the recorded famous speech of Swami Vivekananda at the parliament of the World's Religions in Chicago in 1893. The power spectrum of these nonlinear signals are given by Figs. 1a, 1b, 1c, and 1d respectively. Power spectrum is calculated by FFT method with sampling frequency as 0.50. All of these external signals are nonlinear and non-stationary, established by Surrogate data test [34] and quantile–quantile plot [35] respectively.

Consider the 4D LS system [11] that is used to study the nonlinear basic equations of acoustic gravity waves. This is given by Eq. (4).

$$\left( \frac{dx_1}{dt}, \frac{dx_2}{dt}, \frac{dx_3}{dt}, \frac{dx_4}{dt} \right) = (a(x_2 - x_1) + cx_4, x_1(r - x_3) - x_2, x_1x_2 - bx_3, -x_1 - ax_4); \quad (4)$$

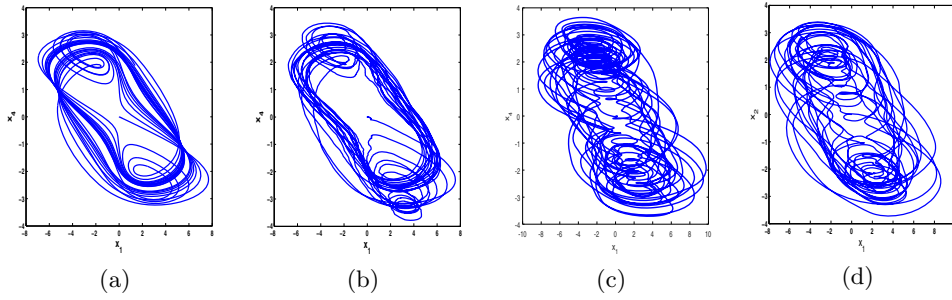


**Fig. 2.** 2D projection of the phase spaces comprising of the solution components  $x_1, x_4$  of (a) 4D LS system, (b) 4D LS system perturbed with two different non-Gaussian noises  $n_1, n_2$ , (c) 4D LS system perturbed with two different music signals  $m_1, m_2$ , (d) music ( $m_1$ ) and speech ( $s_1$ ) signals induced 4D LS system.

$a = 1.0, b = 0.7, c = 1.5, r \in [5, 26]$  and  $x_1(0) = 0.001, x_2(0) = 0.002, x_3(0) = 0.003, x_4(0) = 0.004$ .

Also consider the LS system perturbed with two varieties of power noises  $n_i = \frac{1}{f^{\beta_i}}, i = 1, 2; \beta_1 = 0.5, \beta_2 = 1$ , with two music signals ( $m_1$  and  $m_2$ ) and with one music signal ( $m_1$ ) and another speech signal ( $s_1$ ) with different strengths  $\alpha_1, \alpha_2$  respectively. The general form of the perturbed LS system is given by Eq. (5).

$$\left( \frac{dx_1}{dt}, \frac{dx_2}{dt}, \frac{dx_3}{dt}, \frac{dx_4}{dt} \right) = (a(x_2 - x_1) + cx_4 + \alpha_1 V_1, x_1(r - x_3) - x_2, x_1x_2 - bx_3 + \alpha_2 V_2, -x_1 - ax_4). \quad (5)$$

For noise induced LS system,  $V_1 = n_1, V_2 = n_2, \alpha_1 = 5.5, \alpha_2 = 5.2$ ; for the LS system perturbed with two different music signals,  $V_1 = m_1, V_2 = m_2, \alpha_1 = 0.001, \alpha_2 = 0.002$ ; for the LS system perturbed with a combination of music and speech signals,  $V_1 = m_1, V_2 = s_1, \alpha_1 = 0.001, \alpha_2 = 0.002$ .

The parameter values  $a, b, c, r$  and the initial conditions remain same as the 4D LS system given by Eq. (4).

The 2D projection of the 4D LS system and all of the perturbed systems show a chaotic regime. However, the nature of the 2D projection of the phase spaces are not exactly similar for all values of  $r$  lying in the range [5, 27]. In other words, the system changes its complex behavior with its parameter  $r$ , which is not possible to identify from the projection of their phase spaces and even from their WRP 's. As sample illustration, the 2D projection of the 4D phase space of the LS system, noise induced LS system, music signals induced LS system and music-speech induced LS system comprising of the solution components  $x_1$  and  $x_4$  for the parameter value  $r = 26$  are given by Figs. 2a, 2b, 2c and 2d respectively. The corresponding WRP are shown by Figs. 3a, 3b, 3c and 3d respectively.

In order to find the changes in complexity, the WRPE  $H(r)$  is computed for each  $r$  in all of the above cases. These are given by Figs. 4a, 4b, 4c and 4d respectively.

It is evident from Fig. 4a that initially for  $r = 5$ , the complexity of the LS system is low (close to 3.4) and then it gradually increases and settle down to the range [3.7, 3.9] with few fluctuations for the higher values of  $r$ . This indicates that the LS system was less complex initially for  $r = 5$ . However, it becomes more complex with the increase in the value of the system parameter  $r$  with few exceptions. Figure 4b indicates that the complex behavior of noise perturbed LS system remains almost

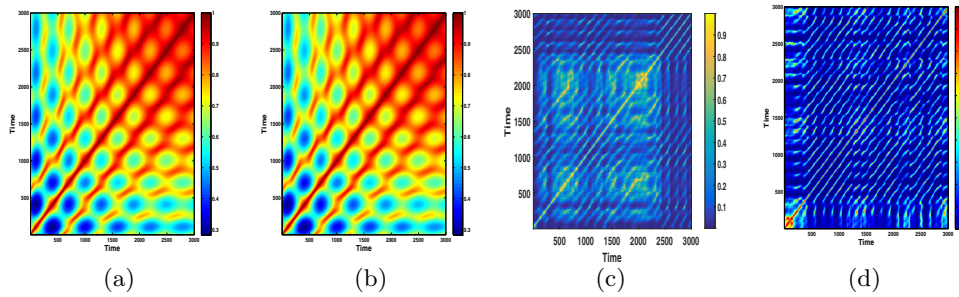


**Fig. 3.** WRP for (a) 4D LS system, (b) 4D LS system perturbed with two different non-Gaussian noises  $n_1, n_2$ , (c) 4D LS system perturbed with two different music signals  $m_1, m_2$ , (d) music ( $m_1$ ) and speech ( $s_1$ ) signals induced 4D LS system.

similar to that of the LS system. For LS system perturbed by two different music signals the complexity is sufficiently high from the initial stage i.e., for  $r = 5$ . With the increase in the value of the system parameter  $r$ , the complexity decreases and again increases frequently. As a whole, the system behaves less complex especially for the higher values of  $r$  (Fig. 4c). In case of music-speech induced LS system, the complexity graph is quite similar to that of the same for two different music signals induced LS system with the exception that in this case the fluctuation of complexity is less frequent (Fig. 4d).

For a better visualization of the changes of complexity in the aforesaid four cases of LS system with respect to the parameter  $r \in [5, 26]$ , we combined the complexities obtained in each cases to form a contour plot. This is given by Fig. 4e.

Furthermore, we have observed the changes in complexity in the aforesaid three perturbed systems for a fixed value of the system parameter  $r$  with respect to the two different strengths  $\alpha_1, \alpha_2$  of the external signals (noise, music and speech signals). This is given by Fig. 5. It is evident from Fig. 5 that the strength parameter  $\alpha_2$  influences the complexity of the perturbed LS system more than  $\alpha_1$ . For the noise perturbed LS system, the complexity is comparatively less for lower values of  $\alpha_2$  ( $\alpha_2 \in (0.001, 0.005)$ ), for music signals perturbed LS system the complexity is comparatively less again for lower values of  $\alpha_2$  ( $\alpha_2 \in (0.001, 0.003)$ ), while it is comparatively less for higher values of  $\alpha_2$  ( $\alpha_2 \in (0.008, 0.01)$ ) in case of music-speech perturbed LS systems.

### 3 Measure of synchronization

Synchronization is basically an adjustment of rhythms of oscillating objects due to their weak interactions. The specific synchronized motion that emerges for identical systems is complete synchronization (CS). This is considered as the most natural synchronization state corresponding to the equality of the state variables of the two systems while they evolve in time. In this article since we have considered only the 4D LS system and perturbed the system in different ways by noise, music and speech signals, it is, therefore, more convenient to study complete synchronization (CS). Geometrically, CS corresponds to the collapse of the complete systems trajectory in the phase space onto an identity hyperplane (known as synchronization manifold).

#### 3.1 Synchronization error analysis

In Pecora and Carroll [32, 33] coupling scheme known as PC configuration, complete synchronization between a response system and its replica was investigated by

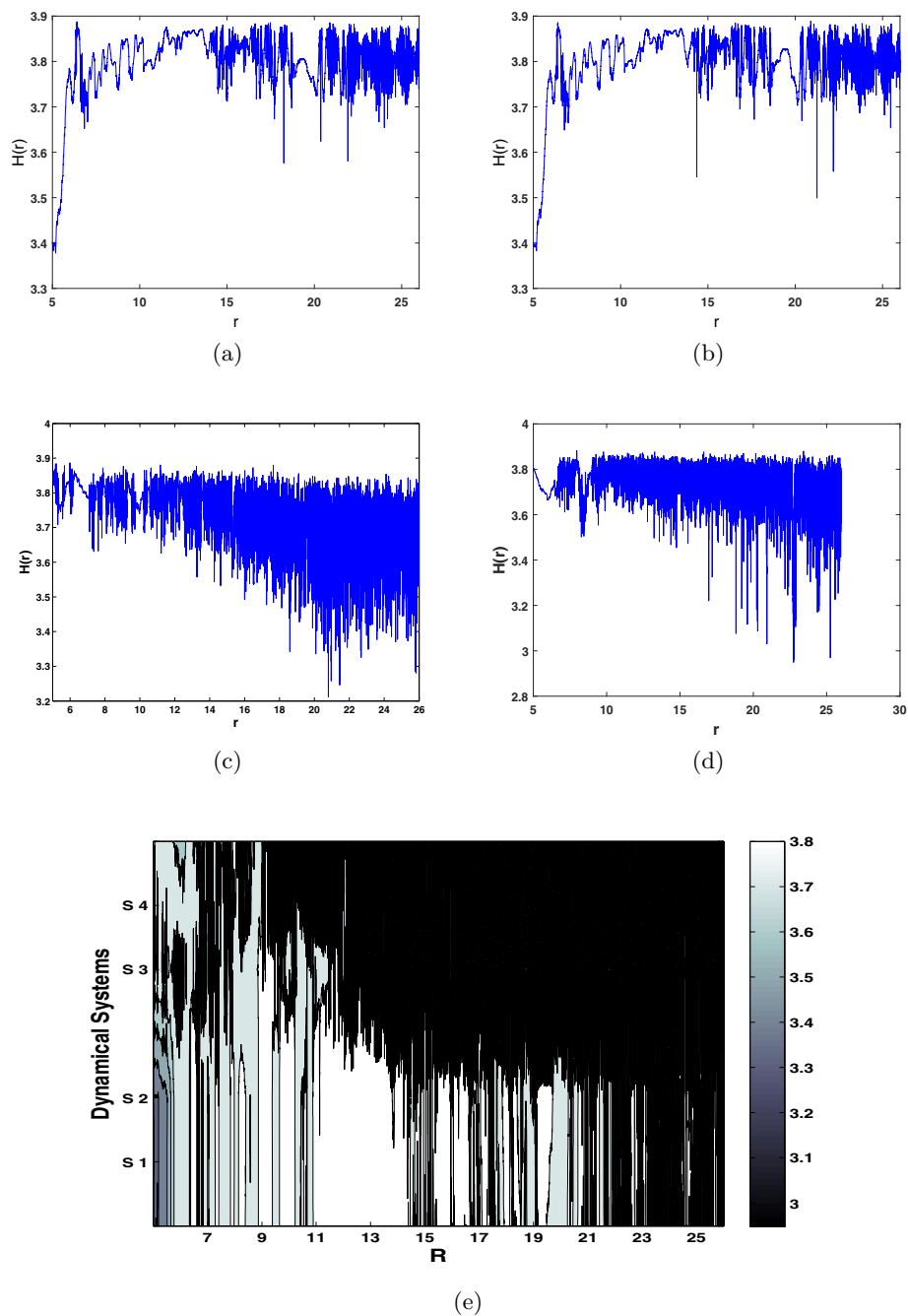


**Fig. 4.** Graph of WRPE  $H(r)$  for  $r = 26$  with respect to the parameter  $r$  for (a) 4D LS system, (b) 4D LS system perturbed with two different non-Gaussian noises  $n_1, n_2$ , (c) 4D LS system perturbed with two different music signals  $m_1, m_2$ , (d) music ( $m_1$ ) and speech ( $s_1$ ) signals induced 4D LS system, and (e) Contour plot of WRPE,  $H(r)$  of 4D LS system ( $S_1$ ) and perturbed LS system with two different non-Gaussian noises ( $S_2$ ), perturbed LS with two different music signals  $m_1, m_2$  ( $S_3$ ), perturbed LS with a combination of music ( $m_1$ ) and speech ( $s_1$ ) signals ( $S_4$ ).

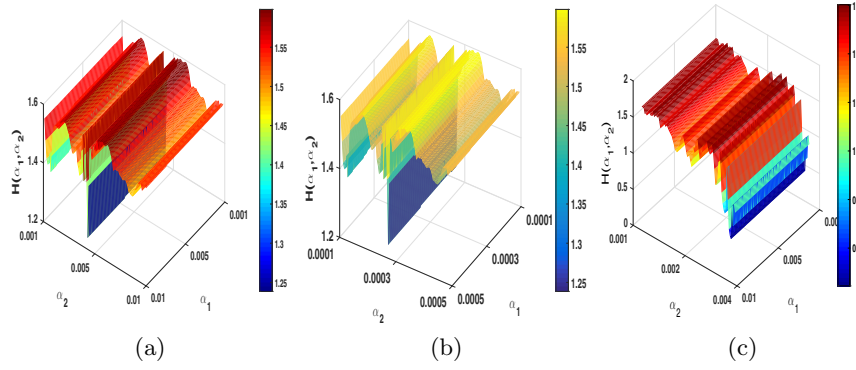


**Fig. 5.** Graph of WRPE  $H(\alpha_1, \alpha_2)$  for  $r = 26$  with respect to the parameter  $\alpha_1, \alpha_2$  for (a) 4D LS system perturbed with two different non-Gaussian noises  $n_1, n_2$ , (b) 4D LS system perturbed with two different music signals  $m_1, m_2$ , (c) music ( $m_1$ ) and speech ( $s_1$ ) signals induced 4D LS system, Both of  $\alpha_1, \alpha_2$  are taken in the range of  $[0.001, 0.01]$  with a step length of 0.0001.

measuring the synchronization error between them. In fact, this is an alternative way to check complete synchronization. In PC configuration, synchronization error (SE) is defined as the norm of the difference between the system and its replica. For complete synchronization (CS),  $SE \rightarrow 0$  as  $t \rightarrow \infty$ . Thus, in order to test the existence of CS between two identical coupled systems, we compute synchronization error with respect to the coupling strength. For this purpose, we consider the perturbed LS system given by (5) as driver and its replica (Eq. (6)) as response system.

$$\left( \frac{dy_1}{dt}, \frac{dy_2}{dt}, \frac{dy_3}{dt}, \frac{dy_4}{dt} \right) = (a(y_2 - y_1) + cy_4 + \alpha_1 V_1 + C(x_1 - y_1), y_1(r - y_3) - y_2, y_1 y_2 - by_3 + \alpha_2 V_2, -y_1 - ay_4); \quad (6)$$

$a = 1.0, b = 0.7, c = 1.5, r \in [5, 26]$  and  $y_1(0) = 0.0015, y_2(0) = 0.0025, y_3(0) = 0.0035, y_4(0) = 0.0045$ . In Eq. (6),  $C$  denotes the coupling strength.

For noise induced LS system,  $V_1 = n_1, V_2 = n_2, \alpha_1 = 5.5, \alpha_2 = 5.2$ ; for the LS system perturbed with two different music signals,  $V_1 = m_1, V_2 = m_2, \alpha_1 = 0.001, \alpha_2 = 0.002$ ; for the LS system perturbed with a combination of music and speech signals,  $V_1 = m_1, V_2 = s_1, \alpha_1 = 0.001, \alpha_2 = 0.002$ .

The change in SE with the increase of coupling strength and time in the aforesaid three types of perturbed LS system is shown by Figs. 6a, 6b and 6c respectively. The corresponding normalized synchronization error (NSE) is shown by Fig. 6d.

It clearly follows from Figs. 6a, 6b, 6c that synchronization error (SE) is more in case of noise induced LS system than music signals induced and speech music induced LS systems. However in each case, this error gradually decreases with the increase in the coupling strength ( $C$ ). This is confirmed in Fig. 6d, which shows that as the coupling strength increases the normalized synchronization error (NSE) tends to zero in all the three cases. Thus the system and its replica tend to a completely synchronous state for higher coupling strength in each of the above three cases.

### 3.2 Mean Conditional Recurrence (MCR)

Whenever there is synchronization between two systems, one of the interesting phenomena is to observe the complex coupling between them. Sometimes this coupling



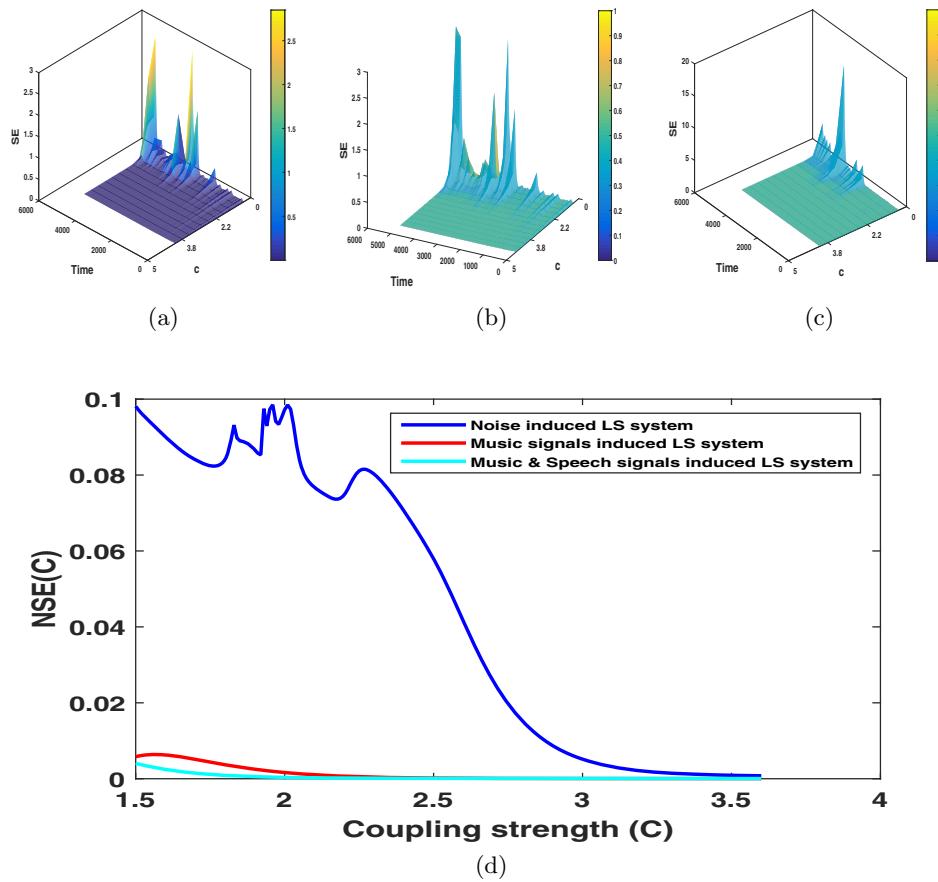


**Fig. 6.** Surface plots describing the changes in Synchronization error (SE) with respect to the coupling strength  $C$  and time for (a) noise perturbed 4D LS system, (b) music signals induced 4D LS system, (c) music and speech signals induced 4D LS system, (d) Plot of NSE against the coupling strength  $C$  for (a), (b), and (c).

is found to be symmetric and in most of the cases it is asymmetric in nature. In the later case, it is, therefore, important to find the driver and response system. Mean Conditional Recurrence (MCR) introduced by Romano et al. is the most promising tool in this context. MCR is basically the mean conditional probabilities of recurrence between the systems  $X$  and  $Y$  (say). MCR involves the concept of Recurrence Plot (RP) and Joint Recurrence Plot (JRP).

The recurrence between any two points  $x_1, x_j \in R^n$  means how much they are closed to each other in that phase space. Mathematically,  $x_1, x_j \in R^n$  are recurrent if  $x_j \in N_\epsilon(x_1)$ , where  $\epsilon$  is a proper threshold. RP is diagrammatic representation of the matrix  $R_{i,j} = \Theta(\epsilon - \|x_i - x_j\|)$ ,  $i = 1, 2, \dots, N$ , where  $\|\cdot\|$ , is the Euclidean norm in  $\mathfrak{R}^n$  and  $\Theta$  is the Heaviside function. Thus,  $R_{i,j} = 1$ , if  $x_j \in N_\epsilon(x_i)$  and 0, otherwise. In RP, 1 and 0 are represented by black and white dots respectively. Therefore, recurrence of any two points in  $n$ -dimensional phase space is visualized as a black spot in 2D RP.

On the other hand, Joint Recurrence Plot (JRP) is the pictorial representation of the Joint recurrence matrix  $JR_{i,j}^{XY} = \Theta(\epsilon_X - \|x_i - x_j\|)\Theta(\epsilon_Y - \|y_i - y_j\|)$ ,  $i = 1, 2, \dots, N$ , where  $\epsilon_X, \epsilon_Y$  be the thresholds for the systems  $X, Y$  respectively. Unlike

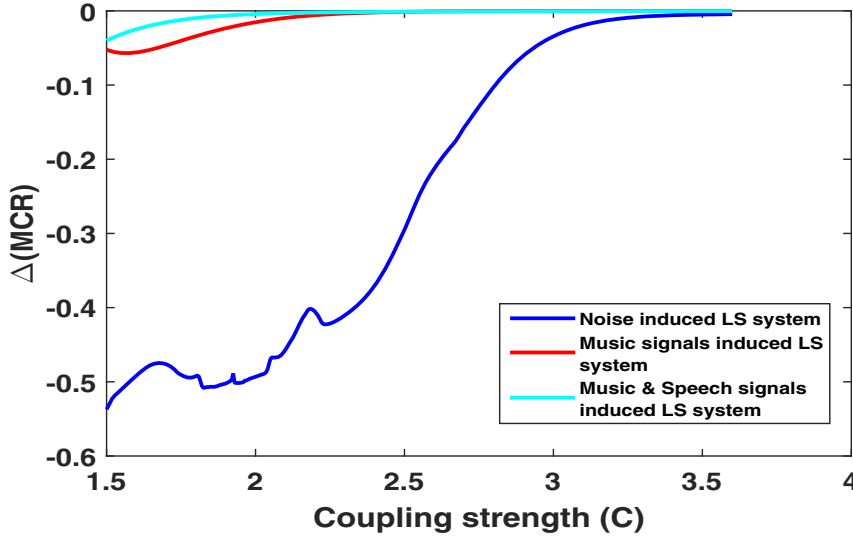


**Fig. 7.** Plot of  $\Delta(MCR)$  with respect to the coupling strength  $C$  in noise perturbed, music signals induced and music, speech signals induced LS system synchronization.

RP, JRP considers the recurrence of two systems  $X, Y$  simultaneously. JRP can be used in measuring different kind of complex coupling. In fact, JRP can also be used to detect generalized synchronization (GS), a stronger type of synchronization. However, as far as direction of coupling is concerned, JRP alone cannot recognize the driver and response system. Thus it is used jointly with RP to find the driver and response systems in an asymmetric coupling scheme.

### 3.3 Detection of driver-response systems by Mean conditional recurrence

Mathematically, Mean conditional recurrence (MCR) of the system  $X$  with respect to  $Y$  and that of the system  $Y$  with respect to  $X$  are respectively defined as

$$MCR(X|Y) = \frac{1}{N} \sum_{i=1}^N \frac{\sum_{j=1}^N JR_{ij}^{XY}}{\sum_{j=1}^N R_{ij}^Y}, MCR(Y|X) = \frac{1}{N} \sum_{i=1}^N \frac{\sum_{j=1}^N JR_{ij}^{XY}}{\sum_{j=1}^N R_{ij}^X}, \quad (7)$$

where  $R_{i,j}^X = \Theta(\epsilon_X - \|x_i - x_j\|)$ ,  $R_{i,j}^Y = \Theta(\epsilon_Y - \|y_i - y_j\|)$ ,  $i = 1, 2, \dots, N$ .

To detect the asymmetry of the coupling, the following criteria is being used:

$$\begin{aligned} \Delta(MCR) &= MCR(X|Y) - MCR(Y|X), \\ \Delta(MCR) > 0 &\Rightarrow X \text{ drives } Y, \\ \Delta(MCR) < 0 &\Rightarrow Y \text{ drives } X. \end{aligned} \quad (8)$$

However if  $\Delta(MCR) = 0$ , the coupling is symmetric.

For the noise induced LS system, we have considered  $X$  as the noise induced LS system and  $Y$  as its replica. In case of music signals perturbed LS system,  $X$  is taken as the music signals perturbed LS system, while  $Y$  represents its replica. On the other hand,  $X$  is considered as music and speech signals induced LS system and  $Y$  as its replica for the music and speech signals induced LS system. Figure 7 shows the change of  $\Delta(MCR)$  with the coupling strength  $c$  for each of the three perturbed systems.

It is observed from Fig. 7 that, an asymmetric coupling exist initially in all of the three cases. However, as coupling strength increases the asymmetric nature of the coupling rapidly decreases and getting symmetric. This tendency is comparatively high for the music signals perturbed LS system and music and speech signals induced LS system. In a more details, for the music signals perturbed LS system and speech signals induced LS system, the coupling becomes symmetric after  $c = 1.9$ , while for noise induced LS system symmetric coupling is detected after  $c = 3.3$ . It is also verified from Fig. 6 that in all of the three cases, the replica systems act as response system.

## 4 Conclusions

In this article, we have first investigated the change in complexity of a stochastic dynamical system induced by noise and various nonlinear signals by the entropy of the weighted recurrence plot. In the next part of the analysis, the complete synchronization (CS) between two systems induced by noise/signals are investigated with proper coupling. The nature of the coupling has also been detected by mean conditional recurrence(MCR). Numerical results show the variation of normalized synchronization errors and MCR with the different choice of speech and music signals as well as various noises. Future scopes include but not limited to its practical implementation for the purpose of system identification.

This research is funded by Vietnam National Foundation for Science and Technology Development (NAFOSTED) under grant number 102.02-2012.27.

## References

1. C.E. Shannon, Bell Syst.Tech. J. **27**, 379423 (1948)
2. Y.G. Sinai, Dokl. Akad. Nauk. SSSR **124**, 768771 (1959)
3. A. Kolmogorov, Dokl. Akad. Nauk. SSSR **124**, 754755 (1959)
4. S. Pincus, Proc. Natl. Acad. Sci. **88**, 22972301 (1991)
5. J. Richman, J. Moorman, Am. J. Physiol. **278**, 9 (2000)
6. N. Packard, J. Crutchfield, D. Farmer, R. Shaw, Phys. Rev. Lett. **45**, 712716 (1980)
7. F. Takens, Dynamical Systems and Turbulence, Lecture Notes in Mathematics **898**, edited by D.A. Rand and L.-S. Young (Springer-Verlag, 1981), p. 366381
8. S.K. Palit, S. Mukherjee, D.K. Bhattacharya, Neurocomputing **113**, 4957 (2013)
9. S.K. Palit, S. Mukherjee, D.K. Bhattacharya, Appl. Math. Comp. **218**, 89518967 (2012)
10. M.B. Kennel, R. Brown, H.D.I. Abarbanel, Phys. Rev. A **45**, 34033411 (1992)
11. S. Banerjee, P. Saha, A. Roy Chowdhury, Phys. Scrip. **63**(3), 177 (2001)
12. J.S. Iwanski, E. Bradley, Chaos **8**, 861871 (1998)
13. E. Bradley, R. Mantilla, Chaos **12**, 596600 (2002)
14. M. Thiel, M.C. Romano, P.L. Read, J. Kurths, Chaos **14**, 234243 (2004)
15. Y. Zou, M. Romano, M. Thiel, J. Kurths, Recurrence Quantification Analysis, edited by C.L. Webber, Jr. and N. Marwan (2015), p. 6599
16. N. Marwan, N. Wessel, U. Meyerfeldt, A. Schirdewan, J. Kurths, Phys. Rev. E **66**(2), 026702 (2002)
17. H. Rabarimanantsoa, L. Achour, C. Letellier, A. Cuvelier, J.-F. Muir, Chaos **17**, 013115 (2007)
18. C. Letellier, H. Rabarimanantsoa, L. Achour, A. Cuvelier, J.-F. Muir, Phil. Trans. Royal Soc. London A: Math., Phys. and Engg. Sci. **366**, 62163 (2008)
19. C. Letellier, Phys. Rev. Lett. **96**, 254102 (2006)

20. D. Eroglu, T.K.D. Peron, N. Marwan, F.A. Rodrigues, L.d.F. Costa, M. Sebek, I.Z. Kiss, J. Kurths, *Phys. Rev. E* **90**(4), 042919 (2014)
21. S. Mukherjee, S.K. Palit, S. Banerjee, M.R.K. Ariffin, L. Rondoni, D.K. Bhattacharya, *Physica A* **439**, 93 (2015)
22. S. Banerjee, *Chaos Synchronization and Cryptography for Secure Communications: Applications for Encryption* (IGI Global, 2010)
23. H. Fujisaka, T. Yamada, *Prog. Theor. Phys.* **72**(5), 885 (1984)
24. V.S. Afraimovich, N.N. Verichev, M.I. Rabinovich, *Radiofizika* **29**(9), 1050 (1986)
25. L.M. Pecora, T.L. Carroll, *Phys. Rev. Lett.* **64**, 821 (1990)
26. N.F. Rulkov, M.M. Sushchik, L.S. Tsimring, H.D.I. Abarbanel, *Phys. Rev. E* **51**, 980 (1995)
27. L. Kocarev, U. Parlitz, *Phys. Rev. Lett.* **76**, 1816 (1996)
28. M.G. Rosenblum, A.S. Pikovsky, J. Kurths, *Phys. Rev. Lett.* **76**, 1804 (1996)
29. E.R. Rosa, E. Ott, M.H. Hess, *Phys. Rev. Lett.* **80**, 1642 (1998)
30. M.C. Romano, M. Thiel, J. Kurths, C. Grebogi, *Phys. Rev. E* **76**, 036211 (2007)
31. N. Marwan, M.C. Romano, M. Thiel, J. Kurths, *Phys. Rep.* **438** (2007)
32. L.M. Pecora, T.L. Carroll, *Phys. Rev. Lett.* **64**, 821 (1990)
33. L.M. Pecora, T.L. Carroll, *Phys. Rev. A* **44**, 2374 (1991)
34. H. Kantz, T. Schreiber, *Nonlinear Time Series Analysis* (Cambridge University Press, 2004), p. 334
35. W.L. Martinez, A.R. Martinez, *Computational Statistics Handbook with Matlab* (Chapman & Hall/CRC, 2002)